# REPORT DOCUMENTATION PAGE

Form Approved
OMB NO. 0704-0188



1. AGENCY USE ONLY ( Leave Blank)

2. REPORT DATE 28 FEB 2003

3. REPORT TYPE AND DATES COVERED
Final Progress Report: 1 Aug 2002 – 31 Jan 2003

4. TITLE AND SUBTITLE
Projectile Base Flow Analysis

5. FUNDING NUMBERS
44013-EG-II, Contract No. DAAD1902C0063

6. AUTHOR(S)
David C. Wilcox

7. PERFORMING ORGANIZATION NAME(S) AND ADDRESS(ES)
DCW Industries, Inc.
5354 Palm Drive
La Canada, CA 91011

8. PERFORMING ORGANIZATION REPORT NUMBER
DCW-38-R-05

9. SPONSORING / MONITORING AGENCY NAME(S) AND ADDRESS(ES)

U. S. Army Research Office
P.O. Box 12211
Research Triangle Park, NC 27709-2211

10. SPONSORING / MONITORING AGENCY REPORT NUMBER

11. SUPPLEMENTARY NOTES
The views, opinions and/or findings contained in this report are those of the author(s) and should not be construed as an official Department of the Army position, policy or decision, unless so designated by other documentation.

12 a. DISTRIBUTION / AVAILABILITY STATEMENT

Approved for public release; distribution unlimited.

12 b. DISTRIBUTION CODE

13. ABSTRACT (Maximum 200 words)

The primary purpose of this research project has been to analyze, through detailed plots and analysis, results obtained in ARO Contract DAAD19-99-C-0047. We have also determined model-predicted effects of base bleed on projectile base flows.

In clarifying the impact of model revisions made to the Wilcox Stress-ω model in Contract DAAD19-99-C-004, we have revised and improved surface boundary conditions for both the Stress-ω and k-ω models.

Detailed mean-flow and turbulence-property profile plots show that the k-ω model predictions are closer to measurements than those of the Stress-ω model and those of computations done by other researchers using the k-ε model. A grid resolution study confirms that the numerical results obtained in our computations are accurate.

Numerical experiments seeking improvements in predicted results using the Stress-ω model failed to achieve any significant improvement. Attempts to improve k-ω model predictions with a nonlinear stress/Strain-rate constitutive relation also proved ineffective.

Predictions for effects of base bleed are consistent with measurements and are similar to those obtained in other research studies.

14. SUBJECT TERMS

15. NUMBER OF PAGES
13

16. PRICE CODE

| 17. SECURITY CLASSIFICATION OR REPORT | 18. SECURITY CLASSIFICATION ON THIS PAGE | 19. SECURITY CLASSIFICATION OF ABSTRACT | 20. LIMITATION OF ABSTRACT |
|---|---|---|---|
| **UNCLASSIFIED** | **UNCLASSIFIED** | **UNCLASSIFIED** | **UL** |

# 1. Introduction

In Contract DAAD19-99-C-004, numerical simulation of projectile base flows yielded promising results. Differences between computed and measured base pressure and reattachment points over a range of Mach and Reynolds numbers were acceptably small for most design studies [Wilcox (2001)]. On balance, a modified version of the Wilcox Stress-$\omega$ model [Wilcox (1998)] predicted averaged base pressure a bit closer to measurements than the $k$-$\omega$ model.

However, in order to achieve the improved results with the Stress-ω model and to improve numerical stability, we modified the production term in the $\omega$ equation. Specifically, we made the following replacement.

$$\alpha \frac{\omega}{k} \tau_{ij} \frac{\partial u_i}{\partial x_j} \rightarrow \alpha S_{ij} S_{ji} \tag{1}$$

In Equation (1), $\alpha$ is a closure coefficient, $\omega$ is specific dissipation rate, $\tau_{ij}$ is the specific Reynolds-stress tensor, $u_i$ is the velocity vector, $x_j$ is the position vector and $S_{ij}$ is the mean strain-rate tensor. We made no assessment of the proper value for the closure coefficient $\alpha$ in Contract DAAD19-99-C-004.

This study accomplished five things.

1. It focused on the appropriateness of the model modification quoted in Equation (1).
2. It examined details of one of the computations done in Contract DAAD19-99-C-004.
3. It did a grid-resolution study to confirm the accuracy of the computation analyzed in detail.
4. It attempted improvements to the Stress-ω model and tested a nonlinear stress/strain-rate constitutive relationship with the $k$-$\omega$ model.
5. It made computations for effects of base bleed.

Section 2 describes the first part of our analysis addressing the question of the appropriate value for $\alpha$. We discovered that the surface boundary condition for both the Stress-$\omega$ and $k$-$\omega$ models can be improved in a way that improves the accuracy of both models for boundary layers. We also discovered that no choice of the coefficient $\alpha$ exists that warrants the change in the production term.

Section 3 includes detailed plots of velocity and turbulence-property profiles and comparison with corresponding measurements for the Herrin-Dutton, Mach 2.5 base flow experiment [Herrin-Dutton (1994)]. It also summarizes results of a grid-resolution study.

Section 4 discusses attempts to improve the Stress-$\omega$ model and to implement a nonlinear stress/strain-rate constitutive relationship with the $k$-$\omega$ model.

Section 5 presents new results in which base bleed has been included.

# 2. Surface Boundary Conditions

Whenever a turbulence model is modified, it should be retested for turbulent flow data against which the model was originally calibrated. One set of data for which both the Stress-$\omega$ and $k$-$\omega$ models have been calibrated is the viscous sublayer. In particular, in analyzing the sublayer, we have devised surface boundary conditions for both models that are appropriate for both smooth and rough surfaces.

As noted in the Introduction, we found in Contract DAAD19-99-C-004 that the Stress-$\omega$ model's predictions and numerical stability for base flows improve by revising the production term in the $\omega$ equation. However, while the production-term revision appeared to be an improvement to the model, we had not verified that the revision is satisfactory for all of the other flows to which the Stress-$\omega$ model has been applied.

In this research project, we found from study of the viscous sublayer and attached boundary layers that the closure coefficients would have to be a bit different from those used in the original model. In doing the analysis, we made a remarkable discovery regarding surface boundary conditions.

The original Stress-$\omega$ model used surface boundary conditions that are somewhat different from those appropriate for the $k$-$\omega$ model [Wilcox (1998)]. In analyzing the new version of the Stress-$\omega$ model, we conclude that both models should use exactly the same boundary condition for both smooth and rough surfaces. Specifically, for both models, the surface value of $\omega$ is given by

$$\omega = \frac{u_\tau^2}{\nu} S_R \quad \text{at} \quad y = 0 \tag{2}$$

where the dimensionless quantity $S_R$ is the following function of the dimensionless roughness height defined by $k_s^+ = u_\tau k_s/\nu$ ($k_s$ is the physical surface-roughness height).

$$S_R = \begin{cases} (200/k_s^+)^2, & k_s^+ \le 5 \\ 25(10/k_s^+)^6, & 5 \le k_s^+ \le 12.4 \\ 85/k_s^+, & k_s^+ \ge 12.4 \end{cases} \tag{3}$$

For very smooth surfaces, we can deduce from these equations that the appropriate surface boundary condition (the so-called "slightly-rough-wall" boundary condition) is given by

$$\omega = \frac{40000\nu_w}{k_s^2} \quad \text{at} \quad y = 0 \tag{4}$$

The figure below shows the effect of surface roughness on model-predicted skin friction, $c_f$, for boundary layers at both Mach 5 and for incompressible conditions. As shown, consistent with measurements, there is no noticeable effect of roughness when $k_s^+$ is less than 5. The results, which are virtually identical for the $k$-$\omega$ and Stress-$\omega$ models, are clearly consistent with the measurements of Reda, Ketter and Fan (1974).

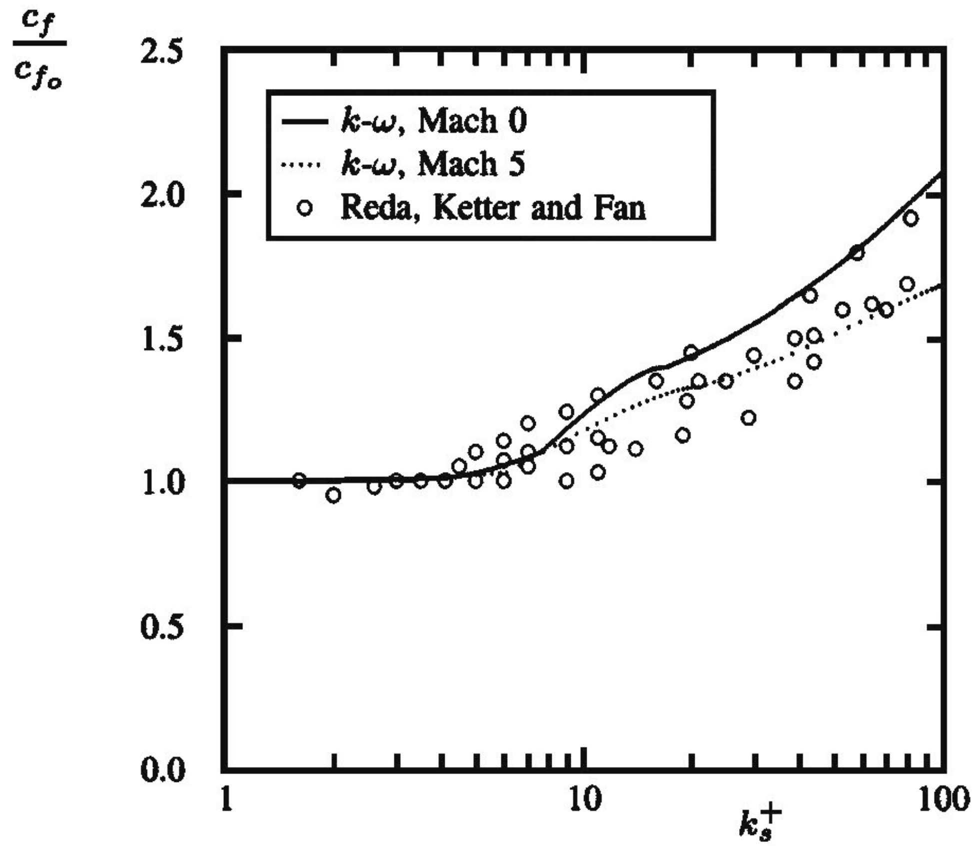


***Figure 1: Computed and measured effects of surface roughness on skin friction for compressible turbulent boundary layers.***

Interestingly, the boundary condition described in Equations (2) – (4) is essentially independent of the revised production term in the $\omega$ equation.

Moving on to attached boundary layers and homogeneous turbulent flows, it quickly became obvious that changing the production term as described in Equation (1) had an undesirable effect on model predictions for these baseline test cases. No value of the closure coefficient $\alpha$ exists that preserves the model's integrity. Consequently, the modification described in Equation (1) must be rejected.

# 3. Detailed Analysis of a Mach 2.5 Projectile Base Flow

A central task of this project was to analyze results of the $k$-$\omega$ and Stress-$\omega$ model computations performed for base flows in Contract DAAD19-99-C-0047. Specifically, the goal has been to make plots throughout the near-wake region of the Herrin-Dutton, Mach 2.5 base flow and compare computed and measured flow properties.

Figure 2 compares computed and measured horizontal-velocity profiles, $u/U_\infty$, at four stations downstream of the base. Table 1 summarizes the measurement locations and the computed and measured centerline stagnation point locations.

**Table 1. Measurement Stations and Stagnation-Point Locations**

| Item | $x/D$ |
|---|---|
| **Measurement Station 1** | **1.26** |
| **Stagnation Point: $k$-$\omega$** | **1.29** |
| **Stagnation Point: Measured** | **1.32** |
| **Measurement Station 2** | **1.42** |
| **Stagnation Point: Stress-$\omega$** | **1.43** |
| **Measurement Station 3** | **1.73** |
| **Measurement Station 4** | **1.89** |
| **Stagnation Point: RNG $k$-$\varepsilon$** | **1.93** |

## 3.1 Horizontal-Velocity Profiles

As shown in Figure 1, the $k$-$\omega$ model's horizontal velocity profiles are quite close to measured values at the first two Measurement Stations. This is consistent with the fact that these two profiles straddle the measured centerline stagnation point, and that the $k$-$\omega$ model's stagnation point also lies between Measurement Stations 1 and 2. By contrast, the Stress-$\omega$ model's stagnation point lies just downstream of Measurement Station 2 so that greater discrepancies are expected.

Both models' predictions are far closer to measurements than the RNG $k$-$\varepsilon$ model as implemented by Sahu (1994). The RNG $k$-$\varepsilon$ model predicts a stagnation point that lies downstream of all four Measurement Stations, corresponding to a recirculation region much greater in extent than measured.

At the two Measurement Stations farther downstream of the base, the $k$-$\omega$ model's predicted horizontal velocities are 15%-20% smaller than measured, while those of the Stress-$\omega$ model are 20% to 25% smaller than measured. This is typical of RANS turbulence-model predictions for reattaching flows, i.e., the computed approach to a new equilibrium state is slower than observed experimentally.

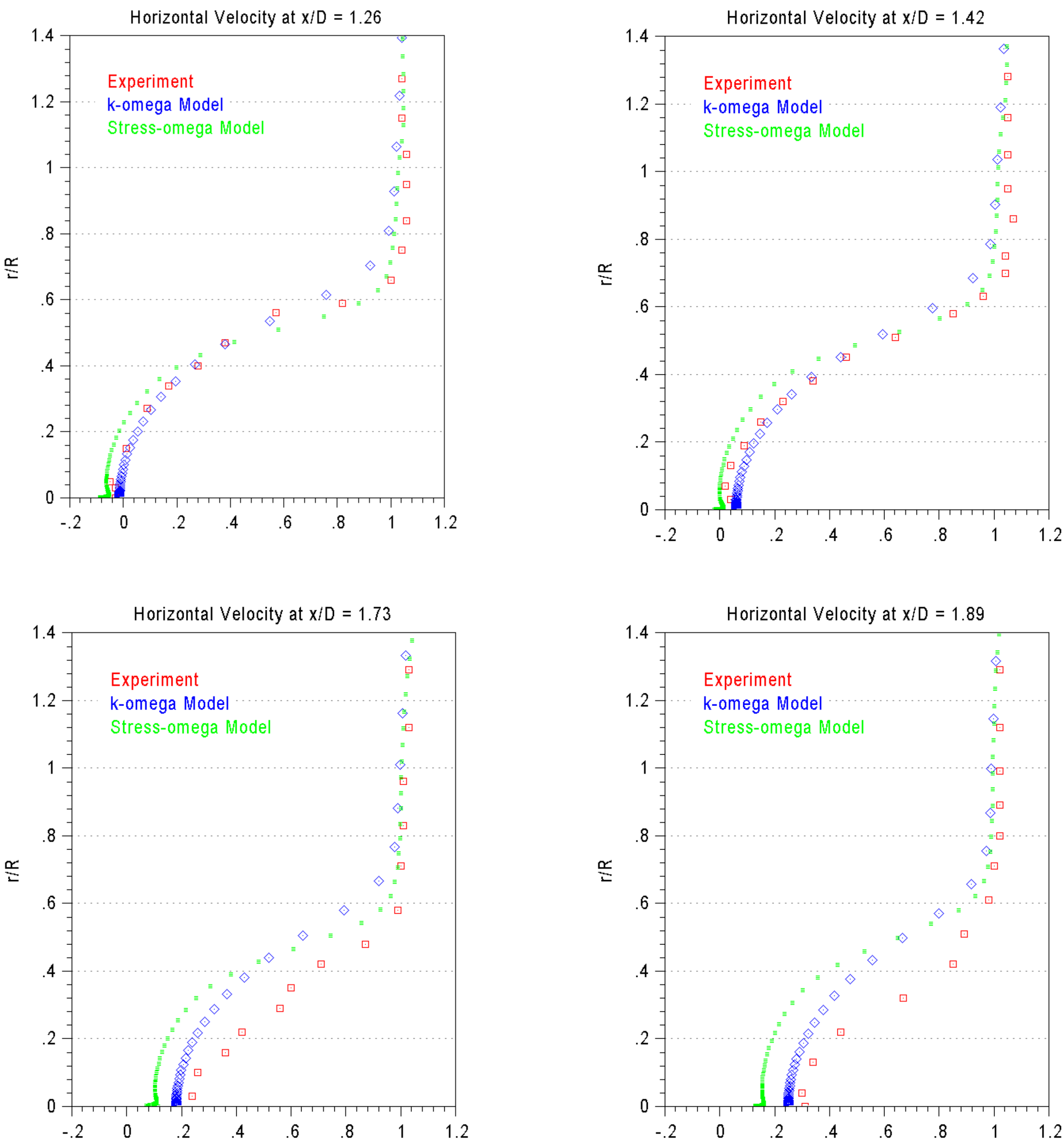


***Figure 1. Comparison of computed and measured horizontal velocities downstream of the base for the Herrin-Dutton, Mach 2.5 flow past an axisymmetric body with a square-cut base.***

# 3.2 Radial Velocity Profiles

Figure 2 compares computed and measured radial-velocity profiles. The most noteworthy difference between computed and measured flowfields is shown in the location of the reattachment shock. The measured profiles at $x/D$ = 1.26 and $x/D$ = 1.42 both show a sharp change in the magnitude of the radial velocity near $r/R$ = 0.6. Farther downstream at $r/R$ = 1.73 the rapid change occurs near $r/R$ = 0.9, while it is off scale at $x/D$ = 1.89.

By contrast, the $k$-$\omega$ model fails to predict abrupt changes in radial velocity. Although the Stress-$\omega$ model does predict sudden changes in radial velocity, the changes occur at about twice the measured distance from the centerline. Since the Stress-$\omega$ model computation required finer resolution near the centerline than the $k$-$\omega$ model computation, the absence of abrupt changes in radial velocities suggests the possibility of inadequate resolution of the flowfield. Inspection of contour plots clearly indicates formation of a reattachment shock for the $k$-$\omega$ model computation.

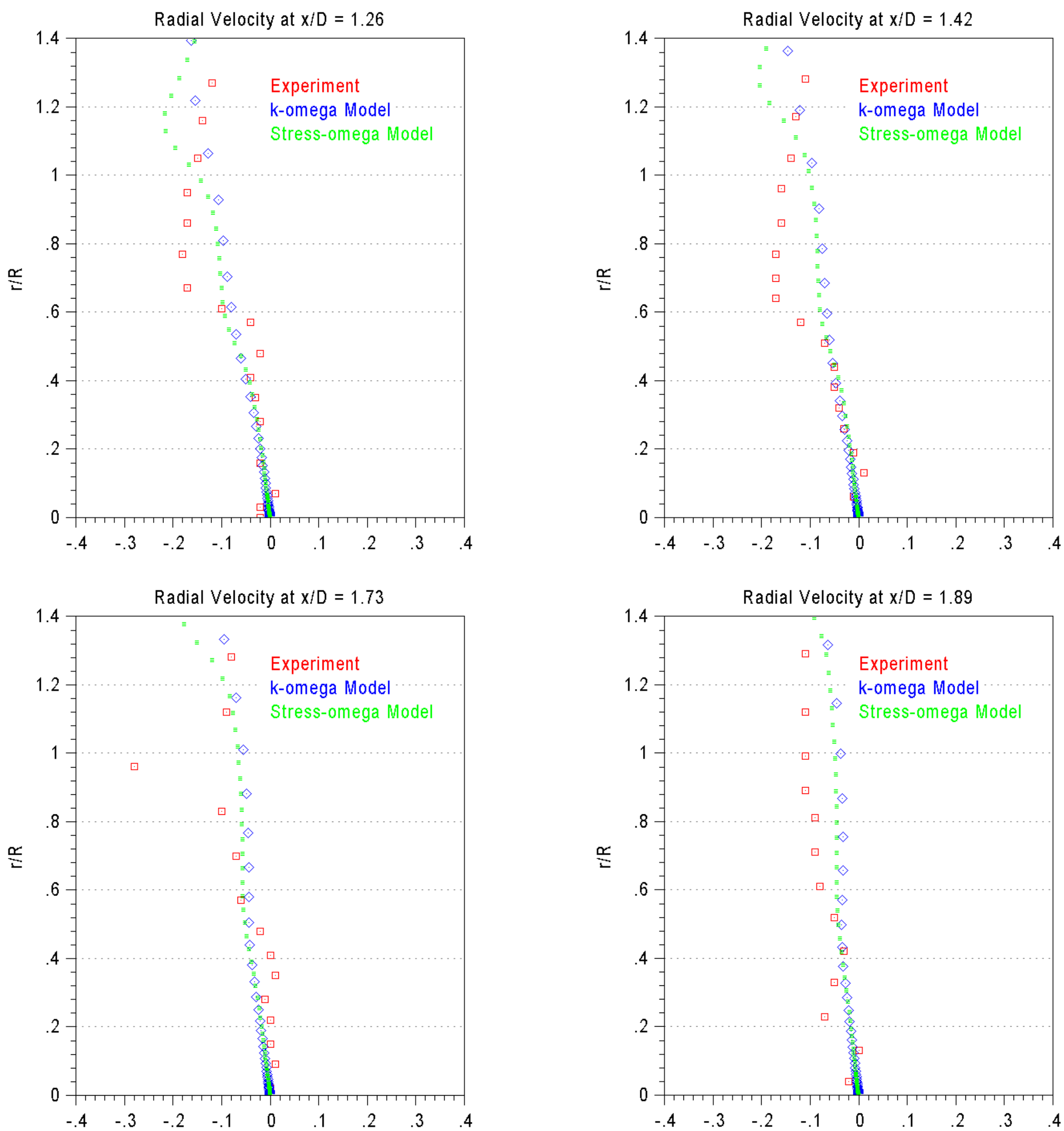


***Figure 2. Comparison of computed and measured radial velocities downstream of the base for the Herrin-Dutton, Mach 2.5 flow past an axisymmetric body with a square-cut base.***

## 3.3 Turbulence Profiles

Figures 3 and 4 compare computed and measured turbulence kinetic energy, $k/U_\infty^2$, and Reynolds shear stress, $<-u'v'>/ U_\infty^2$, throughout the near-wake. Both models fail to predict turbulence kinetic energy profiles that are close to the measured profiles. However, inspection of the Reynolds shear stress profiles reveals a remarkable result. The *k-ω* model's shear stresses are much closer to measured stresses than those of the Stress-*ω* model. This is the reason the velocities are closer as well.

As will be discussed in Section 4 below, rerunning the Stress-*ω* model computations with several adjustments in closure coefficient values and surface boundary conditions yields no significant reduction in differences between computed and measured flow properties.

Nevertheless, both models yield a large improvement in predictive accuracy relative to the *k-ε* model. While base pressure varies with radius, the average value is within a few percent of the measured value. The model thus provides an accurate prediction of body drag. Also, the reattachment length differs from the measured length by just 2%.

## 3.4 Grid-Resolution Study

To investigate the possibility that the *k-ω* computation might have insufficient grid resolution, we repeated the computation with four times as many grid points. The original computation used 200 grid points in the streamwise direction and 160 points between lower and upper mesh boundaries. We generated a grid with 400 streamwise points and 320 points in the other direction.

Changes in major structural features such as base pressure and location of the centerline stagnation point are hardly distinguishable. Richardson extrapolation indicates that, overall, the numerical results are within 3-4% of the continuum solution. Hence, we conclude that the results shown in Figures 1-4 are accurate.

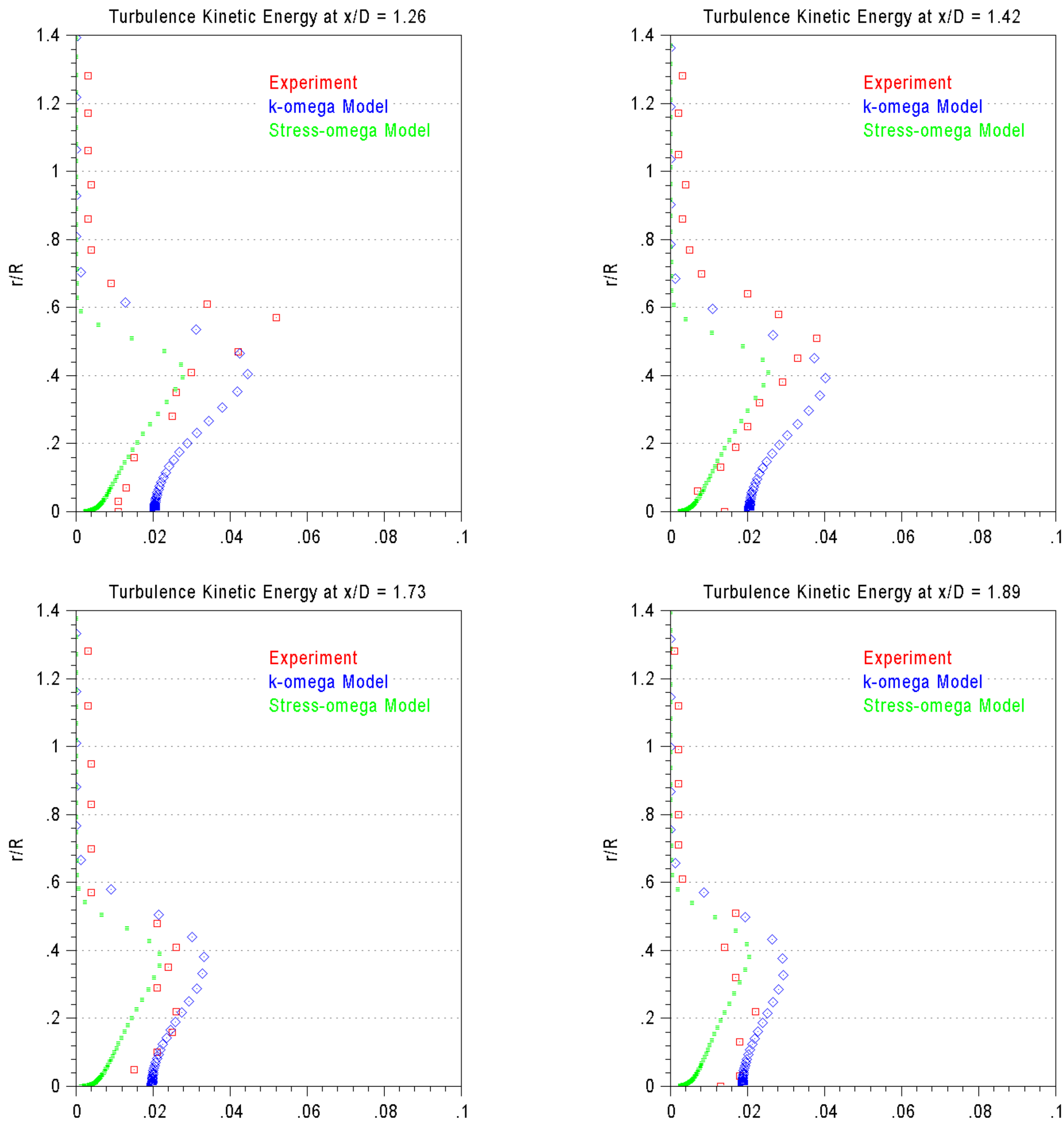


***Figure 3. Comparison of computed and measured turbulence kinetic energy profiles downstream of the base for the Herrin-Dutton, Mach 2.5 flow past an axisymmetric body with a square-cut base.***

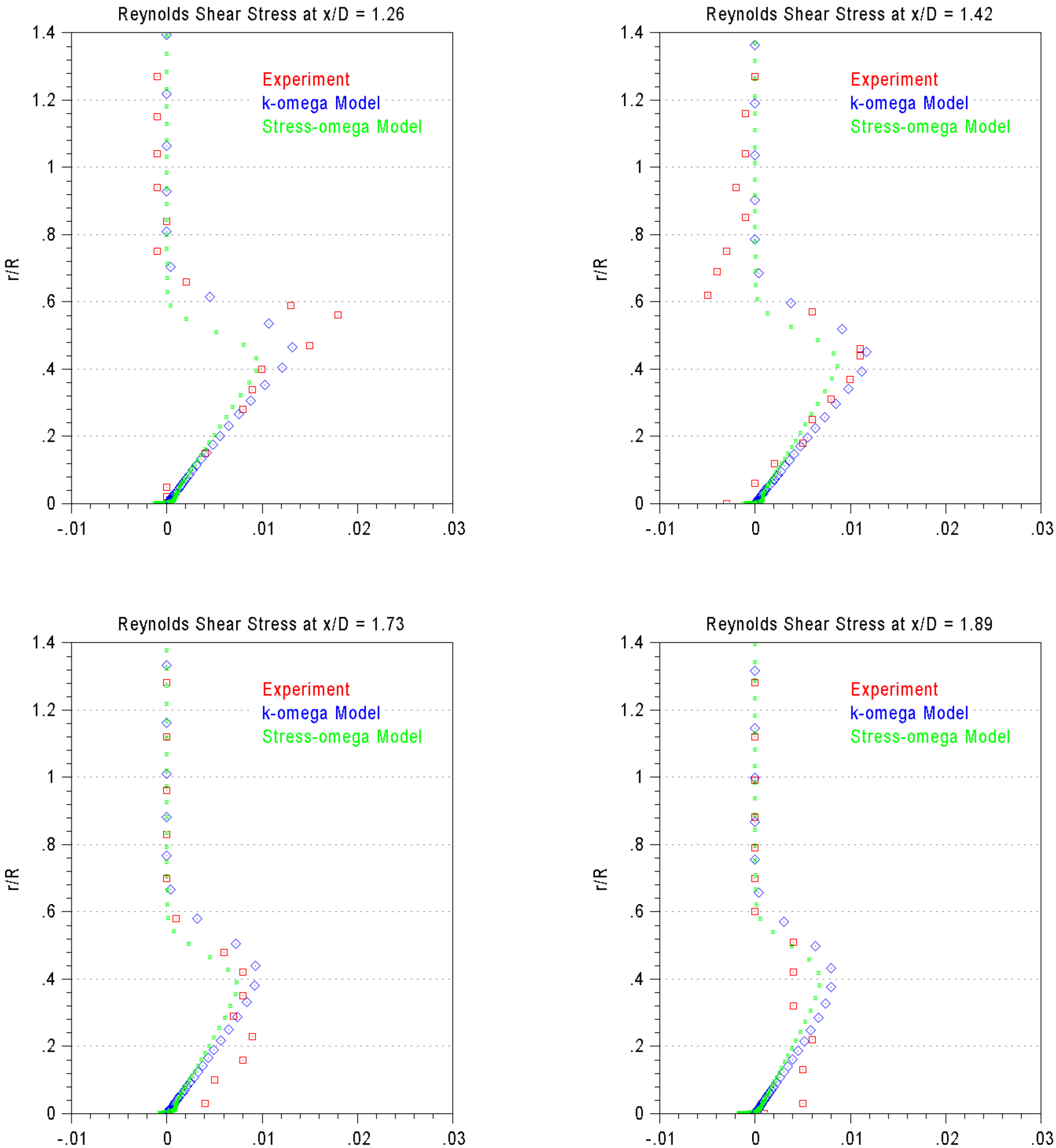


*Figure 4. Comparison of computed and measured turbulence Reynolds shear stress profiles downstream of the base for the Herrin-Dutton, Mach 2.5 flow past an axisymmetric body with a square-cut base.*

# 4. Turbulence-Model Modifications

In an attempt to improve model predictions, we tried two things. First, for the Stress-$\omega$ model, we did numerical experiments with one of the model's key closure coefficients. Second, we used a nonlinear Reynolds-stress/strain-rate constitutive relation with the $k$-$\omega$ model. Neither modification proved fruitful.

## 4.1 Stress-ω Model Revision

One of the terms in the equation governing the Reynolds-stress tensor is known as the "return-to-isotropy" term. It is part of the modeled representation of the pressure/strain-rate correlation tensor that appears in the exact differential equation for the Reynolds stress tensor, $\tau_{ij}$. Specifically, it appears as follows.

$$\rho \frac{d\tau_{ij}}{dt} = -\rho\beta^* C_1 \omega \left( \tau_{ij} + \frac{2}{3} k \delta_{ij} \right) + \ldots \tag{5}$$

In Equation (5) $\rho$ is density, $t$ is time, $\beta^*$ and $C_1$ are closure coefficients, $k$ is turbulence kinetic energy and $\delta_{ij}$ is the Kronecker delta. Of all the closure coefficients in the Stress-$\omega$ model, $C_1$ is the least certain. As argued by Launder, Reece and Rodi (1975), its value can lie within the following range.

$$1.4 \le C_1 \le 1.8 \tag{6}$$

The Stress-$\omega$ model uses a value of $C_1 = 1.8$, which yields optimum results for a wide range of flows.

However, other values of $C_1$ within the entire range specified in Equation (6) yield acceptable results for the baseline test cases that have been used to validate the model. For each value of $C_1$ there is a unique value of the closure coefficient $\alpha$ [see Equation (1)] that preserves the law of the wall, so that in all computations we have done we have simultaneously changed both $C_1$ and $\alpha$.

Disappointingly, varying $C_1$ over the entire range given in Equation (6) yields insignificant changes. The location of the centerline stagnation point, for example, changes by no more than 6%.

## 4.2 k-ω Model Revision

Our second attempt at improving predictive accuracy through model revisions was to use a nonlinear Reynolds-stress/strain-rate constitutive relation. The relation we selected is the Wilcox-Rubesin (1980) formulation in which $\tau_{ij}$ is a quadratic function of the mean-strain rate tensor.

Again, results obtained were disappointing. The most important change was the location of the centerline stagnation point. The use of the nonlinear stress/strain-rate relationship causes the stagnation point to move farther downstream, corresponding to a larger recirculation region. Since the unmodified $k$-$\omega$ model predicts the location to within 2% (see Table 1 in Section 3), this is an undesirable change.

This is consistent with the results obtained by Thangam and Speziale (1992) for flow past a backward-facing step. Use of a nonlinear constitutive relationship with the $k$-$\varepsilon$ and other two-equation models typically increases predicted reattachment location by 10%.

# 5. Effects of Base Bleed

In the final task of the study, we have analyzed effects of base bleed on supersonic flow past a square-based body. We consider flow at two freestream Mach numbers, viz., $M_\infty$ = 1.88 and 2.48 corresponding to the experiments of Bowman and Clayden (1967). For both Mach numbers, the mass-injection parameter, $I$, varies from 0 to 0.02, where

$$I = \frac{\dot{m}_j}{\rho_\infty U_\infty A_b} \quad (7)$$

The quantity $\dot{m}_j$ is the mass flow rate at the bleed exit, $\rho_\infty$ is freestream density, $U_\infty$ is freestream velocity and $A_b$ is the area of the base.

Figure 5 compares computed and measured area-averaged base pressure, $p_b$. Results of $k$-$\varepsilon$ model computations [Sahu (1986)] are included for comparison. As shown, the $k$-$\omega$ results are very similar to those of the $k$-$\varepsilon$ model. For Mach 1.88, both models predict an increase in base pressure that becomes less rapid as $I$ increases. For Mach 2.48, both models predict an initial rise in base pressure followed by a less-rapid-than-observed decrease.

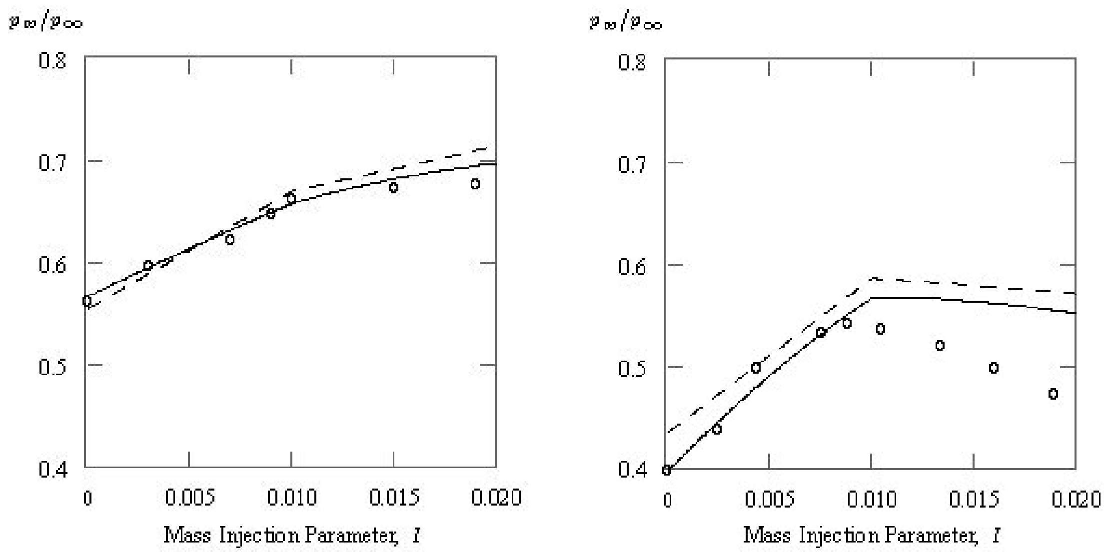


***Figure 5: Computed and measured effects of base bleed on base pressure for freestream Mach numbers of 1.88 (left) and 2.48 (right).* O *Measured, Bowman and Clayden;* —— *k-ω model; - - - - k-ε model.***

# 6. Summary and Conclusions

Results of this study and those of the preceding study by Wilcox (2001) show that the *k-ω* model yields predictions for projectile base flows that are much closer to measured properties than the *k-ε* model. The most significant discrepancy between computed and measured flow properties is that, like the *k-ε* model, computed base pressure varies with radial distance from the centerline. The area-averaged value predicted by the *k-ω* model is nevertheless quite close to corresponding measurements for a wide range of Mach and Reynolds numbers.

As a disappointing outcome of the research, results obtained indicate that, without additional model development, the Stress-*ω* model offers only marginal improvement in predictive accuracy over the *k-ω* model. In some cases, the *k-ω* model predicts flow properties closer to measurement than the Stress-*ω* model.

# References


Bowman, J. E. and Clayden, W. A. (1967), "Cylindrical Afterbodies in Supersonic Flow with Gas Injection," *AIAA Journal*, Vol. 5, No. 8, pp. 1524-1525.

Herrin, J. L. and Dutton, J. C. (1994), "Supersonic Base Flow Experiments in the Near Wake of a Cylindrical Afterbody," *AIAA Journal*, Vol. 32, No. 1, pp. 77-83.

Launder, B. E., Reece, G. J. and Rodi, W. (1975), "Progress in the Development of a Reynolds-Stress Turbulence Closure," *Journal of Fluid Mechanics*, Vol. 68, Pt. 3, pp. 537-566.

Reda, D. C., Ketter, F. C., Jr. and Fan, C. (1974), "Compressible Turbulent Skin Friction on Rough and Rough/Wavy Walls in Adiabatic Flow," AIAA Paper 74-574, Palo Alto, CA.

Sahu, J. (1986), "Supersonic Flow Over Cylindrical Afterbodies with Base Bleed," BRL-TR-2742.

Sahu, J. (1994), "Numerical Computations of Supersonic Base Flow with Special Emphasis on Turbulence Modeling," ARL-TR-438.

Thangam, S. and Speziale, C. G. (1992), "Turbulent Flow Past a Backward Facing Step: A Critical Evaluation of Two-Equation Models," *AIAA Journal*, Vol. 30, No. 5, pp. 1314-1320.

Wilcox, D. C. (1998), *Turbulence Modeling for CFD*, Second Edition, DCW Industries, Inc., La Cañada, CA.

Wilcox, D. C. (2001), "Projectile Base Flow Analysis," DCW Industries Final Report DCW38-R-04.

Wilcox, D. C. and Rubesin, M. W. (1980), "Progress in Turbulence Modeling for Complex Flow Fields Including Effects of Compressibility," NASA TP-1517.